Angle-Distribution Relaxation in a Many-Body Orbital System

A coarse-grained Newtonian flattening theorem

Jonathan R. Landers

New York, N.Y.
April 2026

Abstract

We study the evolving distribution of orbital-plane inclinations in a many-body system with a dominant central mass. The exact Newtonian flow does not, by itself, imply convergence of the inclination law. We therefore separate two levels of description. First, after averaging over fast orbital phases and weak interactions, we show that the coarse-grained Newtonian potential induces a quadratic energy penalty for small inclination away from the preferred plane orthogonal to the total angular-momentum axis, yielding a linear restoring term in inclination space. Second, under an overdamped stochastic closure for the slow inclination dynamics, the induced Fokker–Planck equation is an Ornstein–Uhlenbeck model with an explicit stationary Gaussian law and exponential contraction in relative entropy and total variation. We also show that the resulting flattening law should be understood as an asymptotic reduction principle for the long-time geometry of the N-body problem rather than an exact inversion of the full microstate. Representative figures replace the earlier live simulation and emphasize the geometric and statistical content of the model.

1. Setting

The Newtonian N-body problem has always sat at the border between exact law and irreducible complexity. The underlying force law is simple, yet the collective geometry it generates can be intricate enough to resist closed-form description except in very special regimes [1, 2, 3, 4]. The present note focuses on one geometric statistic that survives this tension in a particularly clean way: the distribution of orbital-plane inclinations in a rotating many-body system.

Consider a dominant central mass m_1 and orbiting masses $m_2, \ldots, m_N$. For each orbiting body $k \in \{2, \ldots, N\}$, let

$$\mathbf{r}_k(t) = (x_k(t), y_k(t), z_k(t)) \in \mathbb{R}^3$$

denote its position relative to m_1. In the coarse-grained flattening model below, we do not evolve the instantaneous elevation angle of the particle position. Instead, we track the signed inclination of the body's orbital plane relative to a preferred horizontal plane, denoted by

$$\theta_k(t) \in \left[-\tfrac{\pi}{2}, \tfrac{\pi}{2}\right].$$

The orbital phase of body k evolves separately within that plane. We are interested in the evolving distribution of the plane inclinations $\{\theta_k(t)\}$. If the initial inclinations are uniformly distributed on $[-\pi/2, \pi/2]$, then the initial law is

$$p_0(\theta) = \frac{1}{\pi} \mathbf{1}_{[-\pi/2,\pi/2]}(\theta),$$

and the empirical distribution at time t is

$$p_N(\theta, t) = \frac{1}{N-1} \sum_{k=2}^{N} \delta\big(\theta - \theta_k(t)\big).$$

The full gravitational dynamics are

$$\ddot{\mathbf{r}}_k = -Gm_1 \frac{\mathbf{r}_k}{|\mathbf{r}_k|^3} - G\sum_{\substack{j=2 \\ j\neq k}}^{N} m_j \frac{\mathbf{r}_k - \mathbf{r}_j}{|\mathbf{r}_k - \mathbf{r}_j|^3}, \qquad k = 2, \ldots, N.$$

If Φ_t denotes the induced phase-space flow, the angle distribution at time t is the pushforward of the initial phase-space law through the map $X_0 \mapsto \Theta_k(\Phi_t(X_0))$.

In the pure N-body Hamiltonian setting, there is generally no reason for the inclination law p_t to converge to a limiting distribution p_*. The dynamics transport and distort orbital planes, but do not by themselves provide dissipation or alignment [2, 3, 4]. If one were instead to study the instantaneous elevation angle $\arcsin(z_k/|\mathbf{r}_k|)$, its distribution would oscillate with orbital phase even more strongly.

Nevertheless, the Newtonian many-body system is not geometrically featureless. When the total angular momentum is nonzero, it singles out a natural axis

$$\mathbf{e}_z := \frac{\mathbf{L}_{\text{tot}}}{|\mathbf{L}_{\text{tot}}|},$$

and hence a natural reference plane $\mathbf{e}_z^{\perp}$. In rotating stellar and galactic systems, this kind of distinguished axis is part of the standard large-scale geometry of the problem [5]. The key step below is to coarse-grain the Newtonian dynamics over fast orbital phases and many weak interactions, thereby extracting a smooth mean-field preference for that plane. This produces the restoring geometry used in the effective inclination model while keeping the exact Hamiltonian and the coarse-grained relaxation theorem conceptually distinct.

2. Coarse-Grained Newtonian Midplane Preference

We now identify the Newtonian origin of the preferred plane. After averaging over the fast orbital phases of the surrounding bodies, replace the exact many-body field experienced by one tagged body by a smooth axisymmetric coarse-grained potential $\Phi_{\text{cg}}(R, z)$ about the angular-momentum axis $\mathbf{e}_z$, with symmetry $\Phi_{\text{cg}}(R, z) = \Phi_{\text{cg}}(R, -z)$. This is the point at which the note moves from exact celestial mechanics to an effective mean-field geometry: not because the microscopic dynamics are abandoned, but because the slow inclination sector becomes clearer once the rapidly oscillating structure has been averaged away [6, 5].

Proposition 1. *Assume Φ_{cg} is C^2 near $z = 0$ and satisfies*

$$\Phi_{\text{cg}}(R, z) = \Phi_{\text{cg}}(R, 0) + \frac{1}{2}\nu^2(R)\, z^2 + O(z^4), \qquad \nu^2(R) := \partial_{zz}\Phi_{\text{cg}}(R, 0) > 0.$$

Let a body of mass m move on a nearly circular orbit of radius a whose orbital plane has small inclination θ relative to the midplane $z = 0$. Then the orbit-averaged excess Newtonian potential energy satisfies

$$\Delta\overline{U}(\theta) = \frac{1}{4} m\, \nu^2(a)\, a^2\, \theta^2 + O(\theta^4) = \frac{1}{2} K\, \theta^2 + O(\theta^4),$$

with

$$K = \frac{1}{2} m\, \nu^2(a)\, a^2 > 0.$$

Consequently, the induced restoring term in inclination space is

$$-\partial_\theta \Delta\overline{U}(\theta) = -K\theta + O(\theta^3).$$

Proof. For a small inclination θ, the vertical displacement along the orbit may be written, to leading order, as

$$z(\psi) = a \sin\psi\, \theta + O(\theta^3),$$

where ψ denotes the orbital phase. The orbit-averaged excess potential energy is

$$\Delta\overline{U}(\theta) = m \left\langle \Phi_{\rm cg}(a, z(\psi)) - \Phi_{\rm cg}(a, 0) \right\rangle_\psi .$$

Using the even-in-z expansion of $\Phi_{\rm cg}$ near the midplane gives

$$\Delta\overline{U}(\theta) = \frac{m}{2}\, \nu^2(a) \left\langle z(\psi)^2 \right\rangle_\psi + O(\theta^4).$$

Substituting $z(\psi) = a \sin\psi\, \theta + O(\theta^3)$ yields

$$\left\langle z(\psi)^2 \right\rangle_\psi = a^2\theta^2 \left\langle \sin^2\psi \right\rangle_\psi + O(\theta^4) = \frac{1}{2}\, a^2\theta^2 + O(\theta^4).$$

Therefore

$$\Delta\overline{U}(\theta) = \frac{1}{4}\, m\, \nu^2(a)\, a^2\theta^2 + O(\theta^4),$$

which is the claimed quadratic energy penalty. Differentiating with respect to θ gives the linear restoring term

$$-\partial_\theta \Delta\overline{U}(\theta) = -K\theta + O(\theta^3). \qquad \square$$

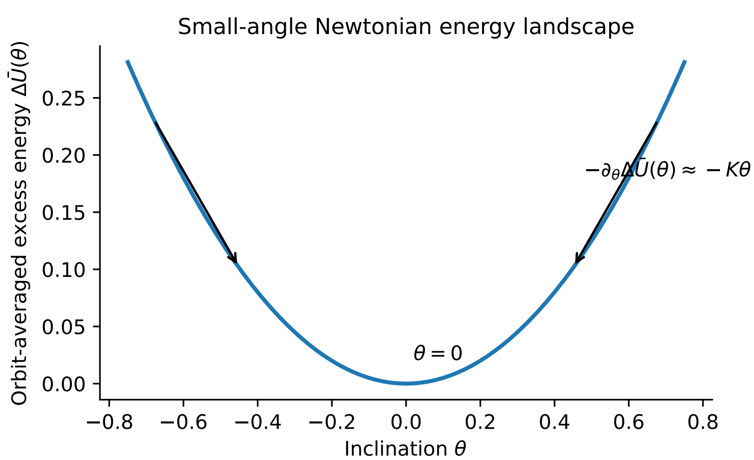

Figure 1: The coarse-grained Newtonian potential induces a quadratic small-angle energy landscape around the preferred midplane. The resulting linear restoring term in inclination space is the small-angle origin of the effective drift used later.

Remark. Proposition 1 identifies the Newtonian origin of the preferred plane and the small-angle restoring geometry. It does not yet imply irreversible convergence of the inclination law. That final step enters only after a coarse-grained closure for the slow inclination dynamics is imposed.

3. Effective Inclination Dynamics

To model the slow inclination sector, introduce the overdamped stochastic closure

$$\dot{\theta} = -\mu\, \partial_\theta \Delta\overline{U}(\theta) + \eta(t),$$

where $\mu > 0$ is an effective mobility and $\eta(t)$ is a mean-zero unresolved forcing term representing weak encounters, phase scrambling, and other perturbative effects. This is the stage at which the geometric preference extracted above is promoted into a statistical law for the angle distribution. Such closures are standard whenever one seeks a tractable description of a slow collective variable while retaining the imprint of the underlying mechanics in the effective coefficients [6, 7, 8]. Linearizing Figure 1 at small angle and writing $\eta(t) = \sqrt{2D}\,\xi(t)$ with white noise ξ, we obtain

$$d\Theta_t = -\kappa\, \Theta_t\, dt + \sqrt{2D}\, dW_t, \qquad \kappa := \mu K > 0.$$

The corresponding Fokker–Planck equation for the angle density $p(\theta, t)$ is

$$\partial_t p = D\, \partial_{\theta\theta} p + \kappa\, \partial_\theta(\theta p), \qquad \theta \in \mathbb{R}.$$

For analytical tractability we have passed from the bounded physical interval $[-\pi/2, \pi/2]$ to an unbounded small-angle approximation $\Theta_t \in \mathbb{R}$, valid when the mass of the distribution concentrates near the midplane and boundary effects are negligible. A bounded-domain model with reflecting boundaries at $\pm\pi/2$ could also be studied, but the unbounded Ornstein–Uhlenbeck setting yields the cleanest closed-form theorem [7, 8].

4. Main Theorem

The payoff of the reduction is that the inclination sector now falls into a class of diffusion models whose convergence theory is explicit. In the present setting, the entire relaxation story can be read directly from the stationary Gaussian and its entropy dissipation [9, 10, 11].

Theorem 1. *Let $p(\theta, t)$ evolve according to the Fokker–Planck equation above with $\kappa, D > 0$. Then:*

(i) the equation admits the stationary distribution

$$p_*(\theta) = \sqrt{\frac{\kappa}{2\pi D}}\, \exp\!\left(-\frac{\kappa\theta^2}{2D}\right);$$

(ii) the relative entropy decays exponentially:

$$\mathrm{KL}(p_t \,\|\, p_*) \le e^{-2\kappa t}\, \mathrm{KL}(p_0 \,\|\, p_*).$$

Proof. Define $u(\theta, t) = p(\theta, t)/p_*(\theta)$. A direct calculation shows the Fokker–Planck equation may be rewritten as

$$\partial_t p = D\, \partial_\theta (p_*\, \partial_\theta u)\,.$$

Let $H(t) := \mathrm{KL}(p_t \,\|\, p_*) = \int p_*\, u \log u\, d\theta$. Differentiating and integrating by parts,

$$\frac{dH}{dt} = -D \int p_*(\theta)\, \frac{(\partial_\theta u)^2}{u}\, d\theta = -4D \int p_*(\theta)\, \left|\partial_\theta \sqrt{u}\right|^2 d\theta.$$

Since p_* is Gaussian, it satisfies the Gaussian log-Sobolev inequality

$$H(t) \le \frac{2D}{\kappa} \int p_*(\theta)\, \left|\partial_\theta \sqrt{u}\right|^2 d\theta.$$

Combining yields $\frac{dH}{dt} \le -2\kappa H(t)$, and Gronwall's inequality gives the claim. □

5. Corollaries

The theorem makes the contraction visible in two complementary languages: relative entropy, which is natural for the diffusion, and total variation, which speaks more directly to the shrinking of the angle law as a probability distribution.

Corollary 1 (TV contraction)**.** *By Pinsker's inequality,*

$$\mathrm{TV}(p_t, p_*) \le \sqrt{\tfrac{1}{2}\,\mathrm{KL}(p_t \,\|\, p_*)} \le e^{-\kappa t}\sqrt{\tfrac{1}{2}\,\mathrm{KL}(p_0 \,\|\, p_*)}.$$

The angle distribution therefore converges exponentially fast, in total variation, to the stationary Gaussian law.

Corollary 2 (Relaxation time)**.** *For target accuracy $\varepsilon > 0$, define*

$$T_\varepsilon := \inf\{t \ge 0 : \mathrm{TV}(p_s, p_*) \le \varepsilon \text{ for all } s \ge t\}.$$

Then

$$T_\varepsilon \le \frac{1}{\kappa}\,\log\left(\frac{\sqrt{\mathrm{KL}(p_0 \,\|\, p_*)/2}}{\varepsilon}\right).$$

This is the expected spectral-gap scaling: convergence time grows like $\kappa^{-1}\log(1/\varepsilon)$.

6. Uniform Initial Law

If the initial angle law is uniform on $[-a, a]$,

$$p_0(\theta) = \frac{1}{2a}\,\mathbf{1}_{[-a,a]}(\theta),$$

a direct computation yields

$$\mathrm{KL}(p_0 \,\|\, p_*) = \log\left(\frac{\sqrt{2\pi D/\kappa}}{2a}\right) + \frac{\kappa a^2}{6D}.$$

For the natural choice $a = \pi/2$,

$$\mathrm{KL}(p_0 \,\|\, p_*) = \log\left(\frac{\sqrt{2\pi D/\kappa}}{\pi}\right) + \frac{\kappa \pi^2}{24D},$$

and substituting into the previous corollary gives an explicit closed-form bound on T_ε in terms of κ, D, and ε alone. In this sense the note starts with the broadest natural inclination law on the physical interval and ends with a quantitative estimate for how quickly the coarse-grained dynamics erase that initial lack of orientation.

Remark. One may also compare p_t and p_* using Jensen–Shannon or other symmetric divergences. These choices do not automatically improve the bound; the essential ingredient is contraction of the coarse-grained dynamics in some divergence. The KL route above is the cleanest, and Pinsker converts it to TV at no real cost.

7. Reduction of the Long-Time Search Space

The coarse-grained inclination law does not invert the full Newtonian microstate: many distinct phase-space configurations can share the same inclination profile or the same angle density. It nevertheless has analytical value, because once the inclination statistics concentrate near the midplane, the admissible long-time dynamics are forced into a nearly planar regime. In that sense the flattening law is a reduction principle for the asymptotic geometry of the N-body problem, even though it is not an exact closed-form solver for the full microscopic flow. The gain is not omniscience but structure: the system remains nonlinear and many-body, yet its large-scale search space narrows in a mathematically meaningful way [4, 5].

Proposition 2 (Asymptotic reduction, not exact inversion)**.** *Suppose that under the effective inclination dynamics one has*

$$\max_{2\le k\le N} |\theta_k(t)| \le \varepsilon \ll 1, \qquad t \ge T.$$

Then for each orbiting body, the vertical displacement and vertical velocity relative to the preferred midplane satisfy

$$z_k(t) = O\big(a_k\varepsilon\big), \qquad \dot z_k(t) = O\big(v_k\varepsilon\big),$$

where a_k and v_k denote the characteristic orbital scale and speed of body k. Consequently the exact Newtonian Hamiltonian admits, for $t \ge T$, the decomposition

$$H_N(t) = H_{\text{planar}}(t) + O\big(\varepsilon^2\big),$$

where H_{planar} is the Hamiltonian obtained by projecting the bodies onto the preferred plane. Thus the coarse-grained flattening law identifies an asymptotically nearly planar reduced regime of the full system, but does not uniquely determine the in-plane phases, eccentricities, or other microscopic degrees of freedom.

Proof. For a small inclination angle, the geometry of an orbit with characteristic radius a_k gives

$$z_k = O\big(a_k \sin\theta_k\big) = O\big(a_k\varepsilon\big).$$

Differentiating along the orbit yields $\dot z_k = O\big(v_k\varepsilon\big)$, where v_k is the corresponding orbital speed scale. Hence the out-of-plane kinetic contribution is

$$\frac{1}{2}m_k\dot z_k^2 = O\big(m_k v_k^2\varepsilon^2\big).$$

Likewise, for pairwise separations one has

$$|\mathbf{r}_k - \mathbf{r}_j|^2 = |\mathbf{r}_k^{\parallel} - \mathbf{r}_j^{\parallel}|^2 + (z_k - z_j)^2,$$

where $\mathbf{r}_k^{\parallel}$ denotes the planar projection. Since $(z_k - z_j)^2 = O\big(\varepsilon^2\big)$, a Taylor expansion of the Newtonian potential around the planar separation shows that each pairwise potential differs from its planar counterpart by $O\big(\varepsilon^2\big)$, provided the projected separations remain away from collision. Summing the kinetic and potential corrections yields

$$H_N(t) = H_{\text{planar}}(t) + O\big(\varepsilon^2\big).$$

The resulting reduction is therefore geometric and asymptotic: it shrinks the long-time search space to a nearly planar manifold, but it cannot be inverted to recover a unique microscopic Newtonian trajectory from the coarse inclination law alone. □

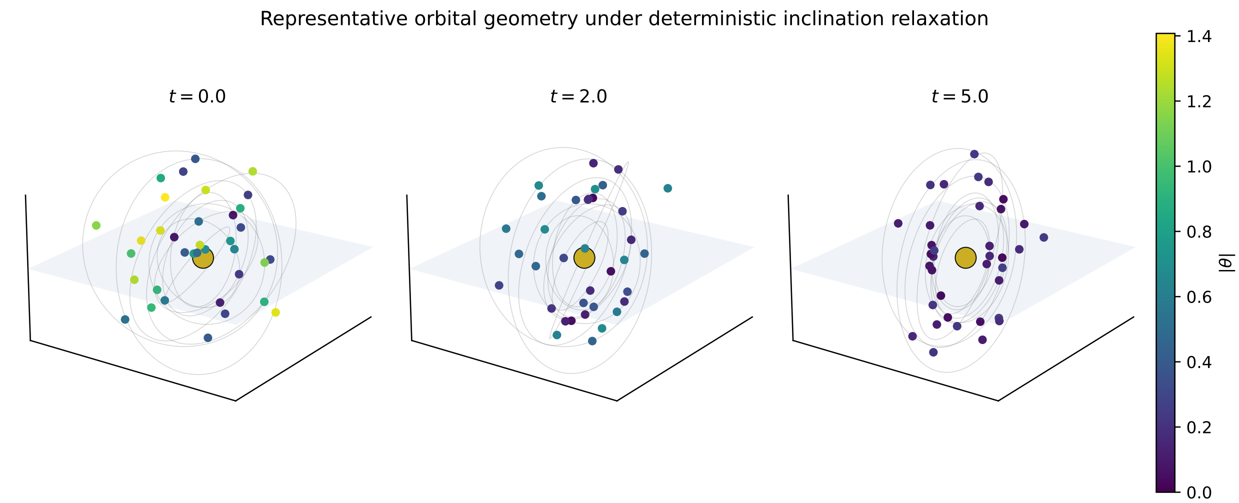

Figure 2: Representative orbital geometry under deterministic inclination relaxation. A sample of initially misaligned orbiters is shown at three times under the visual law $\dot{\theta}_k = -\kappa\theta_k$, with orbital phase evolving on each instantaneous ellipse. The common blue plane is the preferred midplane, and color encodes $|\theta|$. The figure is meant to visualize the geometric flattening component of the coarse-grained model rather than a full microscopic N-body integration.

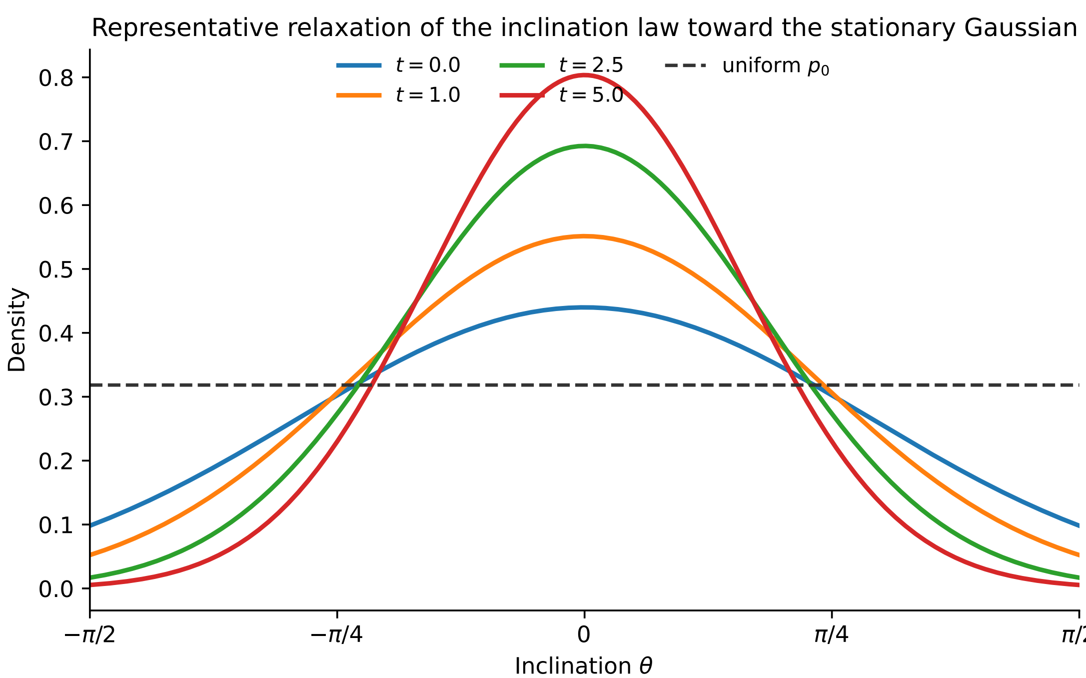

Figure 3: Representative relaxation of the inclination law. Starting from a broad initial profile, the density contracts toward the stationary Gaussian predicted by the Ornstein–Uhlenbeck closure. The dashed curve shows the uniform reference law p_0 on $[-\pi/2, \pi/2]$; the solid curves illustrate increasingly concentrated intermediate profiles.

8. Representative Figures

The original browser-based animation has been replaced by static figures that isolate the two main messages of the note: a geometric flattening of orbital planes toward the preferred midplane, and a statistical concentration of the inclination law toward the stationary Gaussian. These figures are representative of the effective model rather than exact numerical solutions of the microscopic N-body flow.

Taken together, Figures 1 to 3 summarize the narrative arc of the paper: coarse-grained Newtonian geometry creates a preferred midplane and a linear restoring tendency, while the effective stochastic closure upgrades that geometric tendency into a rigorously contractive statistical law. The result is not a full solution of the N-body problem, but it is a compact mathematical story about how one sector of that problem becomes progressively more ordered when viewed at the right scale.

References

[1] I. Newton, *Philosophiae Naturalis Principia Mathematica*, London, 1687.

[2] H. Poincaré, *Les méthodes nouvelles de la mécanique céleste*, Vols. I–III, Gauthier-Villars, Paris, 1892–1899.

[3] A. Wintner, *The Analytical Foundations of Celestial Mechanics*, Princeton University Press, Princeton, 1941.

[4] V. I. Arnold, V. V. Kozlov, and A. I. Neishtadt, *Mathematical Aspects of Classical and Celestial Mechanics*, 3rd ed., Springer, Berlin, 2006.

[5] J. Binney and S. Tremaine, *Galactic Dynamics*, 2nd ed., Princeton University Press, Princeton, 2008.

[6] S. Chandrasekhar, Stochastic Problems in Physics and Astronomy, *Reviews of Modern Physics* **15** (1943), 1–89.

[7] G. E. Uhlenbeck and L. S. Ornstein, On the Theory of the Brownian Motion, *Physical Review* **36** (1930), 823–841.

[8] H. Risken, *The Fokker–Planck Equation: Methods of Solution and Applications*, 2nd ed., Springer, Berlin, 1989.

[9] L. Gross, Logarithmic Sobolev Inequalities, *American Journal of Mathematics* **97** (1975), 1061–1083.

[10] D. Bakry, I. Gentil, and M. Ledoux, *Analysis and Geometry of Markov Diffusion Operators*, Springer, Cham, 2014.

[11] C. Villani, *Hypocoercivity*, Memoirs of the American Mathematical Society **202** (2009), no. 950.